LAWRENCE LIVERMORE NATIONAL LABORATORY

LLNL-JRNL-849724

The observed inefficiency of explosions to produce large aftershocks: Båth's law for explosions is 2.5

S. R. Ford, W. R. Walter

May 31, 2023

Seismological Research Letters

The observed inefficiency of explosions to produce large aftershocks: Båth's law for explosions is 2.5

Sean R. Ford* and William R. Walter

Lawrence Livermore National Laboratory, Livermore, California 94550, USA

* Corresponding author, sean@llnl.gov

August 1, 2023

Declaration of Competing Interests

The authors acknowledge there are no conflicts of interest recorded.

Abstract

Underground explosions are observed to produce fewer and smaller aftershocks than similarly-sized earthquakes. The seismic magnitude difference Δm_{x} between an explosion and its largest aftershock is an expression of Båth's law for explosions. Based on an analysis of a compilation of aftershock studies from Soviet testing at the Semipalatinsk Test Site in Kazakhstan and observations from American testing at the Nevada National Security Site (NNSS), we find that the average magnitude difference for explosions $\overline{\Delta m_{\mathrm{x}}}$ is about 2.5. Based on the NNSS data, two standard deviations of Δm_{x} is about 1.5. In all the cases studied, from ton-to-megaton yield, from shallow-to-overburied depth, and chemical or nuclear source, no explosion aftershock has been larger than the explosion that preceded it. In fact, the two events at the NNSS with

the largest aftershock magnitudes relative to the explosion are associated with the collapse of the cavity created by the explosion. This is similar to observations from North Korean testing at the Punggye-ri Test Site where the largest seismic event following the test is attributed to the collapse after the 2017 explosion and is from 0.8 to 2 magnitude units less than the mainshock.

1 Introduction

Earthquake aftershocks are a well-studied phenomenon that can help in understanding earthquake scaling [e.g., Shearer, 2012] and the total earthquake hazard for a region [e.g., Stein and Liu, 2009]. A well-known empirical constraint on earthquake aftershock distributions is the observation that the largest magnitude aftershock m_{max} is, on average, about one magnitude unit less than the mainshock magnitude m_{main} [e.g., Shcherbakov and Turcotte, 2004]. This constraint on magnitude difference Δm, where $\Delta m = m_{\mathrm{main}} - m_{\mathrm{max}}$, is referred to as Båth's law [Richter, 1958] for Markus Båth [1965] who reported an average value from earthquake observations $\overline{\Delta m_{\mathrm{q}}}$ of 1.2, where the subscript q is to denote the law for earthquakes.

The same physics underlying earthquake aftershocks, namely redistribution of stress following a large rupture, can cause explosion aftershocks. In fact, the locations and mechanisms of explosion aftershocks have been used to understand in-situ crustal stress [Hamilton et al., 1969] and the potential for static stress triggering [Parsons and Velasco, 2009]. However, due to phenomenological differences between earthquakes and explosions – namely the roughly spherical pressurization in the shallow crust versus the faulting along a plane with greater stress increasing with depth – their aftershock distributions can be quite different. These differences have been exploited as a discriminant between explosions and earthquakes [e.g., Ford and Walter, 2010] in nuclear explosion monitoring [for further information on the goals of nuclear explosion monitoring, see the encyclopedia entry by Richards et al., 2019].

Understanding explosion aftershocks can also aid in forensic studies to predict the size and location of an aftershock of a nuclear test, either for on-site inspection [Zucca et al., 1996] or so as not to confuse aftershocks with continued testing [Adushkin et al., 2017]. It is also important in hazard mitigation for explosion monitoring experiments where chemical explosives are used as surrogates to research the seismic effects of nuclear tests. In what follows, we first tell the story of past concerns with explosion-induced seismicity and review a small part of the large body of research done in response to those concerns. Then we take the opportunity to quantify old and new observations of explosion aftershocks making use of relative magnitudes to estimate a "Båth's law for explosions".

1.1 *Superman*, James Bond, and concerns about explosion-induced seismicity

Early in testing it was realized that large explosions can produce aftershocks [Westphal, 1962] and can release in-situ, tectonic strain of the surrounding rock during the explosion process [Brune and Pomeroy, 1963]. The movie, *Superman* [Donner, 1978], exploited these observations with a fiction that a nuclear explosion could cause a large enough earthquake to separate plates at a fault and generate large, destructive aftershocks. In the movie, *A View to a Kill* [Glen, 1985], James Bond foils a plot to simultaneously unlock the Hayward and San Andreas faults with a large bomb. Although the extremes in the movie are the stuff of Hollywood, related ideas were a real concern when testing of megaton-scale weapons was proposed (nuclear test yields are given in tons (t) of TNT, which is an energy unit defined to be exactly 4.184 GJ). In a comment in *Science*, Carter [1969] talked about the potential for the planned megaton-scale nuclear test in Amchitka to trigger a large earthquake. In an interview for the story, J. Brune stated "There is no logical reason why a nuclear explosion couldn't be the initiating event in such a series of events. The larger the explosion, the greater the possibility of its triggering such a series." And later in *Science*, Emiliani et al. [1969] proposed the idea of controlled explosions to release strain, which was followed up in an article titled "Underground Nuclear Explosions: Tectonic Utility and Dangers" by Toksöz and Kehrer [1971] that stated large explosions could release strain energy equivalent to $M > 6$ earthquakes.

The concerns were allayed in the geophysics community after the m_b7 test at Amchitka, named CANNIKIN, when Engdahl [1972] reported small aftershocks with $m_b < 4$ and Willis et al. [1972] reported that "there was no significant change in the pattern of naturally occurring earthquakes following the detonation of this shot." And after Toksöz and Kehrer [1972] looked at the tectonic release for CANNIKIN they found that the non-explosive (tectonic) moment is half the explosion moment, which looks to be about the maximum observed [Howe et al., 2020]. Finally, Richards and Ekström [1995] state, "First, in the 30 year period from 1963-1992, more than 1500 underground tests were carried out (i.e., at a rate of about one test a week). Yet not one of them is associated with either a large earthquake or a destructive earthquake that occurred close to and shortly following the nuclear test."

1.2 Past studies of the largest explosion aftershocks

In the first mentions of maximum explosion aftershock magnitude, Hamilton et al. [1969] state that aftershocks are at least two units of magnitude smaller than the explosion (they reference work by Evernden [1969] presented at the American Geophysical Union Meeting), or $\Delta m_{\mathrm{x}} \geq 2.0$, where the subscript x is to denote the relationship for explosions. As an example, they cite the 1.1 Mt nuclear test, BENHAM [Department of Energy, 2015], which was a M6.3 and its largest aftershock was M4.4 [Hamilton and Healy, 1969]. A similarly reduced maximum aftershock magnitude of about 4.2 was observed for the similarly large magnitude 6.4 Nevada explosion BOXCAR [Ryall and Savage, 1969]. Both BENHAM and BOXCAR were detonated in boreholes more than 1 km deep. In a more extensive analysis of the explosion aftershocks, Hamilton et al. [1972] show that the aftershock series can sometimes be influenced by the collapse of the cavity that was formed by the explosion. Their work suggested that sometimes the largest aftershock could be due to this collapse. This point will be discussed more fully in the Analyses and Discussion sections. Boucher et al. [1969] exploits a more extensive seismic catalog and states, "...it is also worthwhile to point out that all earthquakes so far found to be directly related to underground tests have had magnitudes less, by at least one magnitude unit, than those of the associated blasts." This is in agreement with Douglas [1984] who uses teleseismic catalogs to report that the maximum aftershock magnitude is at least one unit less than the explosion.

Interestingly, the namesake of Båth's law, Markus Båth, commented on induced seismicity like explosions in Båth [1970]. He states, "Thus the three available cases give closely agreeing values of the magnitude difference Δm (= 1.2 in average)... Expressed in energy, it means that even the largest aftershock of an explosion has an energy amounting only to a few percent of the wave energy released in the explosion itself. Such small shocks are almost always harmless." Jarpe et al. [1994] found no correlation between explosive yield and maximum aftershock magnitude. They report results for 4 events and show that the smallest magnitude difference was for the approximately 1 kt chemical explosion conducted for the Non-Proliferation Experiment (NPE) with $\Delta m = 3.6$. Finally, Edwards et al. [1983] looked at the nuclear tests, REDMUD, BILLET, CREWLINE, and LOWBALL and report, "a hint of a relationship exists between nuclear yield and peak event magnitude." We will take the hint and explore the relationship more fully in the next section.

2 Analyses

In order to perform a more quantitative analysis to estimate the average magnitude difference between an explosion and its largest aftershock $\overline{\Delta m_{\mathrm{x}}}$, we will look at data from Soviet testing at the Semipalatinsk Test Site (STS) in Kazakhstan and American testing at the Nevada National Security Site (NNSS).

2.1 Semipalatinsk Test Site (STS)

Adushkin and Spivak [1996] report the maximum aftershock amplitude for a collection of 16 Underground Nuclear Explosion (UNE) aftershock sequences at the STS and nearby Peaceful

Nuclear Explosion (PNE) sites. They find a relationship between the measured amplitude of the largest aftershock a_{max} and the explosion yield w

$$a_{\text{max}} = 2.57w^{0.44}, \tag{1}$$

where the amplitude is in µm/s and yield is in kt. Though they did not provide specifics on the space-time windows for the aftershock association, they did provide an aftershock catalog for the STS UNE Shot 1352 that gives the measured amplitude a and effective magnitude m_{eff} for each event. Based on the aftershock catalog we can fit the relationship

$$m_{\text{eff}} = -2.554 + 1.5\log_{10}(a). \tag{2}$$

Using a_{max} from Equation 1 for a in Equation 2 leads to a relationship between the effective magnitude of the maximum aftershock m_{max} and yield w

$$m_{\text{max}} = -1.939 + 0.667\log_{10}(w). \tag{3}$$

To find a function for the magnitude difference Δm_{x} between the explosion and its maximum aftershock magnitude we also need the magnitude of the explosion. Adushkin and Spivak [1996] provide a means of finding the magnitude of an explosion m_{exp} based on its internal energy e

$$m_{\text{exp}} = (\log_{10}(e) - 11.8)/1.5 \tag{4}$$

where the energy is in J, and since 1 kt is defined to be exactly 4184 GJ,

$$m_{\text{exp}} = 0.548 + 0.667\log_{10}(w) \tag{5}$$

Although, this relationship does not provide an absolute magnitude that could be compared with, for example, teleseismic m_{b}, it does provide enough to determine a function for Δm

since it is relative to the aftershock magnitude measurement. This function is

$$\Delta m_{\mathrm{x}} = m_{\mathrm{exp}} - m_{\mathrm{max}} \tag{6}$$

$$= (0.548 + 0.667 \log_{10}(w)) - (-1.939 + 0.667 \log_{10}(w)) \tag{7}$$

$$= 2.487 \tag{8}$$

Therefore, for these STS-area explosions, Båth's law for explosions is about 2.5.

2.2 Nevada National Security Site (NNSS)

Ford and Walter [2010] studied the aftershocks of 202 nuclear explosions at the NNSS between 1968 and 1992 using a catalog for the region from von Seggern and Brune [2000]. Of the 134 tests that produced at least one observed aftershock in a magnitude-dependent spatiotemporal window, none had an aftershock with a magnitude greater than the explosion. The range in magnitude difference was between 0 and 5, and more than 97.5% had a magnitude difference greater than one unit $\Delta m_{\mathrm{x}} > 1$. The spatiotemporal window is the same used in Uhrhammer [1986] where the search radius r in km and time window t_{win} in days are

$$r = \exp(-1.024 + 0.804m) \tag{9}$$

$$t_{\mathrm{win}} = \exp(-2.87 + 1.235m), \tag{10}$$

where m is the explosion magnitude. As a conservative measure we add 15 km to the radius and 60 days to the time window. Figure 1 shows the results for all the events, giving an average Δm_{x} of 2.54 and its standard deviation is 0.71. Therefore, for these NNSS-area explosions, Båth's law for explosions is about 2.5.

As mentioned in the Introduction section, a complicating influence in explosion aftershock behavior is the collapse of the cavity formed during the explosion. There is a cube-root yield dependence on cavity radius, so a larger explosion creates a larger cavity, and a larger cavity, if unstable, could collapse producing a seismic signal that would be positively correlated with its explosive yield. Using the recorded collapse times in Springer et al. [2002] we associated the maximum aftershocks to determine if they were possibly related to a collapse. If they are associated to the collapse then the symbol in Figure 1 is filled. Though there is no general trend in a collapse relationship to maximum aftershock magnitude, we can see that the two events with $0 \leq \Delta m_{\mathrm{x}} < 1$ are the historical UNEs, DAUPHIN and LEYDEN, where the maximum magnitude aftershock is associated with the collapse.

2.2.1 Source Physics Experiment (SPE)

Two campaigns of chemical explosions were conducted for the Source Physics Experiment (SPE) between 2011 and 2019 at the NNSS. These experiments were to study explosion source physics, in particular generation of shear waves by explosions. More general information on the SPE is in Snelson et al. [2013] and many papers have analyzed the results [e.g., Pitarka et al., 2015, Mellors et al., 2018, Pyle and Walter, 2021]. The first phase of the SPE included a series of six chemical explosions, with yields between 1 and 5 tons TNT conducted at borehole U-15N in Climax Stock granite of northern Yucca Flat. Ford [2020] showed that the largest explosion in SPE Phase I, SPE-5, produced small, but measurable aftershocks.

The second phase of the SPE included a series of four chemical explosions with yields between 1 and 50 tons TNT equivalent yield conducted at a deep borehole U-2EZ in the alluvium of Yucca Flat. This second phase of the experiment is referred to as the Dry Alluvium Geology (DAG) campaign. Ichinose et al. [2021] showed that the largest explosion in SPE Phase II, DAG-2, had a very productive aftershock sequence. Information on the largest explosion ("mainshock") and largest aftershock for each Phase of the SPE is in Table 1 and representative recordings of the events are shown in Figure 2. The station choice in the figure was influenced by the fact that recordings of SPE-5 and DAG-2 closer than about 500 m and 1 km, respectively, were clipped. In Figure 2, although the traces are somewhat narrowband, the aftershock waveforms are different from the explosive ones, which is consistent with the aftershocks having different and perhaps more tectonic mechanisms that are not associated with explosions or collapses.

In an exploration of operational approaches to calculating differential magnitude Δm between a mainshock x and aftershock y, Schaff and Richards [2014] showed that the ratio of the ℓ^2-norms works well for low correlation events when the signal-to-noise ratio of the waveforms is approximately the same, such that

$$\Delta m = \log_{10} \frac{\|x\|}{\|y\|}. \tag{11}$$

In practice we use the ratio of root-mean-square of the waveforms, which for the same length window is equivalent to the ratio of their ℓ^2-norms. Δm for the SPE and DAG events are are 3.74 and 2.83, respectively. Note that this is within the 95% range of the historical analysis, which is between 1 and 4 (Figure 1). The aftershock magnitudes in Table 1 are calculated by differencing the calculated differential magnitude from the magnitudes for the SPE chemical explosions reported by the University of Nevada, Reno.

3 Discussion

3.1 Chemical versus nuclear explosion aftershocks

The 1993 NPE explosion directly compared the seismic signal and aftershock behavior of nuclear and chemical explosions at the NNSS, with an analysis reported in Denny [1994]. Seismic waveforms and amplitudes of the two types of events are nearly identical other than a scale factor [e.g., Walter et al., 1994]. This scale factor would result in increased static stress changes at distance, though the distance would be minor owing to the spherical integration of the stress change. In fact, Jarpe et al. [1994] compared the aftershock behavior of the NPE to that of nearby nuclear explosions and found they were essentially identical. We have not found any reported evidence that chemical explosions have different aftershock behavior than nuclear tests when events of similar size and emplacement conditions are compared.

3.2 Background seismicity

In any active tectonic region one also has to consider the possibility that an earthquake would have occurred even without the explosion. This possibility is also a concern for earthquake hazard and we can learn from hazard analysis in the region to assess the probability of background seismicity. As part of the large Yucca Mountain Project [U.S. Department of Energy, 2002] a probabilistic seismic hazard analysis for the Southern Great Basin was performed [Wong and Stepp, 1998]. An input to the analysis is the annual recurrence interval of earthquakes in the region. We employ the curve from Wong et al. [1996] to estimate the probability of background tectonic events in the NNSS region. Figure 3 shows the probability of an earthquake in the region for durations from a day to a year. For example, it is almost certain that within an area of 100 km radius at the NNSS at least one $M3$ earthquake will occur in a year and there is a 50% chance that at least one $M3$ occurs in a month (solid green line). However, if the area is reduced to a radius of 10 km (dashed green line) then the probability drops to around 0.5%. Importantly, the probability of a felt background earthquake of $M \geq 3$ occurring within a 10 km radius and a week after any proposed chemical explosion, though low ($P \lessapprox 0.001$), is nonzero.

3.3 Comparison with earthquake aftershocks

Ford and Labak [2016] fit models to explosion aftershock sequences and found that the ratio of small to large events (b value in Gutenberg-Richter model) and the decay in time (p value in Omori model) are similar to earthquake aftershock sequences, but the productivity of explosion sequences was much lower than earthquake sequences. Jarpe et al. [1994] found similar results for both the NPE and nearby nuclear explosions. This is in agreement with the observations from the aftershock sequence of DAG-2 [Ichinose et al., 2021], but is contrary to the conclusions of Gross [1996]. We hypothesize that this may be due to a lack of completeness in the Gross [1996] catalogs coupled with the additional degrees of freedom that the extended models used in that work provide.

3.4 Insight to North Korean aftershocks

The results obtained here could be used to interpret seismicity from North Korean testing at the Punggye-ri Test Site (PTS). Dodge [2018] performed a comprehensive search for aftershocks near the PTS and found many small events. Taken together the events have a ratio of small to large magnitudes (i.e., the Gutenberg-Richter b-value) similar to earthquake aftershocks and cluster in two compact regions a few kilometers from the PTS. He reports magnitudes for the largest measured aftershocks for the third, fourth, fifth, and sixth declared tests resulting in Δm of approximately 2.2, 2.2, 3, and 1.5, respectively. In their analysis of PTS aftershocks, Adushkin et al. [2017] state that aftershocks from $M5$ explosions in hard-rock are 2-3 magnitude units lower than the source explosion.

The 2017 explosion at the PTS was followed by a large collapse [Liu et al., 2018] with a Δm of 2 based on m_{b}. However, based on regional, intermediate period data the Δm is between 0.8 [Chiang et al., 2018] and 1.4 [Walter et al., 2018]. This analysis combined with the observations of DAUPHIN and LEYDEN shows that large collapses have the potential to create aftershocks with $0 \leq \Delta m < 1$. Importantly, there has never been an observation of an aftershock larger than the explosion ($\Delta m < 0$, which means explosions have never acted as an apparent foreshock).

4 Conclusions

We conclude with the quantitative result that for both the STS and NNSS the average difference in magnitude between the explosion and its largest aftershock is about 2.5. In other words, Båth's law for explosions is 2.5, which is more than a unit of magnitude different than an accepted value for earthquakes of 1.2. Incorporating all the observations at the NNSS gives a mean of 2.54 with standard deviation of 0.71 such that more than 95% of the observations have a Δm_x within 1 to 4. This dataset incorporates kiloton-to-megaton scale explosions that are both normally and deeply buried. This study showed that chemical explosions from the ton size of the SPE to the kiloton size of the NPE behave similarly. Taken together this demonstrates that explosions are inefficient producers of large aftershocks.

It would appear that the reason large explosions do not induce large earthquakes is that the resulting pressurization field is not sustained at great distances from the explosion [Parsons and Velasco, 2009]. This is in contrast to induced earthquakes from industrial operations like wastewater disposal, geothermal energy production, and carbon sequestration [Kroll and Cochran, 2021], where fluid injection and subsequent pressurization of basement faults can occur [Lasocki and Orlecka-Sikora, 2020].

Data and Resources

The earthquake catalog for the NNSS analysis is compiled by von Seggern and Brune [2000] as part of the Yucca Mountain seismic hazard study and is included as part of the CD-ROM companion to Hauk et al. [2004]. The catalog is available from the authors. SPE data is available through assembled datasets at EarthScope (e.g., SPE-5 is assembled dataset 18-024 and DAG-2 is assembled dataset 21-021). All other data used in this paper came from published sources listed in the references.

Acknowledgments

We are grateful for internal reviews by Steve Myers, Moira Pyle, and Qingkai Kong; and two anonymous reviewers whose comments greatly improved the manuscript. This Source Physics Experiment (SPE) research was funded by the National Nuclear Security Administration, Defense Nuclear Nonproliferation Research and Development (NNSA DNN R&D).

The authors acknowledge important interdisciplinary collaboration with scientists and engineers from LANL, LLNL, NNSS, and SNL. This article has been authored by Lawrence Livermore National Security, LLC under Contract No. DE-AC52-07NA27344 with the U.S. Department of Energy.

References

V. V. Adushkin and A. A. Spivak. Characterization of the aftershock emission caused by underground nuclear explosions. *Journal of Earthquake Prediction Research*, 5(4):444–469, November 1996.

V. V. Adushkin, D. I. Bobrov, I. O. Kitov, M. V. Rozhkov, and I. A. Sanina. Remote detection of aftershock activity as a new method of seismic monitoring. *Doklady Earth Sciences*, 473(1):303–307, March 2017. ISSN 1531-8354. doi: 10.1134/S1028334X17030011.

M. Båth. Artificial release of earthquakes. *Scientia*, 105(703):706–724, 1970. ISSN 0036-8687.

Markus Båth. Lateral inhomogeneities of the upper mantle. *Tectonophysics*, 2(6):483–514, December 1965. ISSN 0040-1951. doi: 10.1016/0040-1951(65)90003-X.

Gary Boucher, Alan Ryall, and Austin E. Jones. Earthquakes associated with underground nuclear explosions. *Journal of Geophysical Research (1896-1977)*, 74(15):3808–3820, 1969. ISSN 2156-2202. doi: 10.1029/JB074i015p03808.

James N. Brune and Paul W. Pomeroy. Surface wave radiation patterns for underground nuclear explosions and small-magnitude earthquakes. *Journal of Geophysical Research*, 68 (17):5005–5028, 1963. ISSN 2156-2202. doi: 10.1029/jz068i017p05005.

Luther J. Carter. Earthquakes and Nuclear Tests: Playing the Odds on Amchitka. *Science*, 165(3895):773–776, August 1969. doi: 10.1126/science.165.3895.773.

Andrea Chiang, Gene A. Ichinose, Doug S. Dreger, Sean R. Ford, Eric M. Matzel, Steve C. Myers, and W. R. Walter. Moment Tensor Source-Type Analysis for the Democratic People's Republic of Korea–Declared Nuclear Explosions (2006–2017) and 3 September 2017 Collapse Event. *Seismological Research Letters*, September 2018. ISSN 0895-0695, 1938-2057. doi: 10.1785/0220180130.

Marvin D. Denny, editor. *Proceedings of the Symposium on the Non-Proliferation Experiment: Results and Implications for Test Ban Treaties*. Department of Energy, Rockville, Maryland, April 1994.

Department of Energy. United States Nuclear Tests, July 1945 through September 1992, September 2015. Technical Report DOE/NV–209-REV 16, National Nuclear Security Administration Nevada Field Office, Las Vegas, Nevada, September 2015.

D. A. Dodge. Searching for Induced Seismicity at Punggye-ri Nuclear Test Site Using Subspace Detectors. *Seismological Research Letters*, 89(6):2094–2112, September 2018. ISSN 0895-0695. doi: 10.1785/0220180127.

Richard Donner. Superman, 1978.

A. Douglas. Teleseismic observations of aftershocks immediately following an underground explosion. *Geophysical Journal of the Royal Astronomical Society*, 77(2):503–515, May 1984. ISSN 0956-540X. doi: 10.1111/j.1365-246X.1984.tb01945.x.

C. L. Edwards, M. D. Harper, T. A. Weaver, D. J. Cash, J. M. Ray, and E. F. Homuth. Microquake activity associated with underground nuclear testing at the Nevada Test Site. Technical Report LA-8552-MS, Los Alamos National Laboratory, United States, August 1983.

Cesare Emiliani, Christopher G. A. Harrison, and Mary Swanson. Underground Nuclear Explosions and the Control of Earthquakes. *Science*, 165(3899):1255–1256, September 1969. ISSN 0036-8075, 1095-9203. doi: 10.1126/science.165.3899.1255.

E. R. Engdahl. Seismic effects of the MILROW and CANNIKIN nuclear explosions. *Bulletin of the Seismological Society of America*, 62(6):1411–1423, December 1972. ISSN 0037-1106.

J. F. Evernden. Explosion aftershock magnitudes. *Transactions of the American Geophysical Union*, 50:247, 1969.

Sean R. Ford. Aftershocks of a Chemical Explosion in Granite from the Source Physics Experiment Phase I. Technical Report LLNL-TR-814889, Lawrence Livermore National Laboratory, Livermore, California, September 2020.

Sean R Ford and Peter Labak. An Explosion Aftershock Model with Application to On-Site Inspection. *Pure and Applied Geophysics*, 173(1), 2016. ISSN 0033-4553. doi: 10.1007/s00024-015-1041-x.

Sean R Ford and William R Walter. Aftershock Characteristics as a Means of Discriminating Explosions from Earthquakes. *Bulletin of the Seismological Society of America*, 100(1): 364–376, 2010. ISSN 0037-1106. doi: 10.1785/0120080349.

John Glen. A View to a Kill, 1985.

Susanna Gross. Aftershocks of nuclear explosions compared to natural aftershocks. *Bulletin of the Seismological Society of America*, 86(4):1054–1060, August 1996. ISSN 0037-1106.

R. M. Hamilton and J. H. Healy. Aftershocks of the Benham nuclear explosion. *Bulletin of the Seismological Society of America*, 59(6), December 1969. ISSN 0037-1106.

R. M. Hamilton, F. A. McKeown, and J. H. Healy. Seismic Activity and Faulting Associated with a Large Underground Nuclear Explosion. *Science*, 166(3905):601–604, October 1969. ISSN 0036-8075, 1095-9203. doi: 10.1126/science.166.3905.601.

R. M. Hamilton, B. E. Smith, F. G. Fischer, and P. J. Papanek. Earthquakes caused by underground nuclear explosions on Pahute Mesa, Nevada Test Site. *Bulletin of the Seismological Society of America*, 62(5):1319–1341, October 1972. ISSN 0037-1106.

T F Hauk, J L O'Boyle, S D Ruppert, S. C. Myers, R Abbot, D A Dodge, F Ryall, K. D. Smith, and W R Walter. An Assembled Western United States Dataset for Regional Seismic Analysis. Data Release Report UCRL-TR-206630, Lawrence Livermore National Laboratory, Livermore, California, 2004.

Michael Howe, Göran Ekström, and Paul G. Richards. Vertical force scaling in seismic source models of underground nuclear explosions. *Geophysical Journal International*, 221 (1):251–264, April 2020. ISSN 0956-540X. doi: 10.1093/gji/ggz582.

G. A. Ichinose, S. R. Ford, K. Kroll, D. Dodge, M. Pyle, A. Pitarka, and W. R. Walter. Preliminary Analysis of Source Physics Experiment Explosion-Triggered Microseismicity Using the Back-Projection Method. *Journal of Geophysical Research: Solid Earth*, 126(5), May 2021. ISSN 2169-9313, 2169-9356. doi: 10.1029/2020JB021312.

Steve Jarpe, Peter Goldstein, and J. J. Zucca. Comparison of the Non-Proliferation event aftershocks with other Nevada Test Site events. In *Proceedings of the Symposium on the Non-Proliferation Experiment: Results and Implications for Test Ban Treaties*, Rockville, Maryland, 1994. Department of Energy.

Kayla A. Kroll and Elizabeth S. Cochran. Stress Controls Rupture Extent and Maximum Magnitude of Induced Earthquakes. *Geophysical Research Letters*, 48(11):e2020GL092148, 2021. ISSN 1944-8007. doi: 10.1029/2020GL092148.

Stanislaw Lasocki and Beata Orlecka-Sikora. Anthropogenic Seismicity Related to Exploitation of Georesources. In Harsh K. Gupta, editor, *Encyclopedia of Solid Earth Geophysics*, pages 1–8. Springer International Publishing, Cham, 2020. ISBN 978-3-030-10475-7. doi: 10.1007/978-3-030-10475-7_277-1.

J. Liu, L. Li, J. Zahradník, E. Sokos, C. Liu, and X. Tian. North Korea's 2017 Test and its Nontectonic Aftershock. *Geophysical Research Letters*, 45(7):3017–3025, 2018. ISSN 1944-8007. doi: 10.1002/2018GL077095.

Robert J. Mellors, Arben Pitarka, Eric Matzel, Steven Magana-Zook, Douglas Knapp, William R. Walter, Ting Chen, Catherine M. Snelson, and Robert E. Abbott. The Source Physics Experiments Large N Array. *Seismological Research Letters*, 89(5):1618–1628, June 2018. ISSN 0895-0695. doi: 10.1785/0220180072.

Tom Parsons and Aaron A. Velasco. On near-source earthquake triggering. *Journal of Geophysical Research: Solid Earth*, 114(B10), 2009. ISSN 2156-2202. doi: 10.1029/2008JB006277.

Arben Pitarka, Robert J. Mellors, William R. Walter, Souheil Ezzedine, Oleg Vorobiev, Tarabay Antoun, Jeffery L. Wagoner, Eric M. Matzel, Sean R. Ford, Arthur J. Rodgers, Lewis Glenn, and Mike Pasyanos. Analysis of Ground Motion from An Underground Chemical Explosion. *Bulletin of the Seismological Society of America*, 105(5):2390–2410, 2015. ISSN 0037-1106. doi: 10.1785/0120150066.

Moira L. Pyle and William R. Walter. Exploring the Effects of Emplacement Conditions on Explosion P/S Ratios across Local to Regional Distances. *Seismological Research Letters*, 93(2A):866–879, December 2021. ISSN 0895-0695. doi: 10.1785/0220210270.

Paul G. Richards and Göran Ekström. Earthquake activity associated with underground nuclear explosions. In R. Console and A. Nikolaev, editors, *Earthquakes Induced by Underground Nuclear Explosions: Environmental and Ecological Problems*, volume 4 of *NATO ASI Series*. Springer-Verlag, Berlin, 1995.

Paul G. Richards, Zhongliang Wu, Won-Young Kim, and David P. Schaff. Seismic Monitoring of Nuclear Explosions. In Harsh K. Gupta, editor, *Encyclopedia of Solid Earth Geophysics*, pages 1–14. Springer International Publishing, Cham, 2019. ISBN 978-3-030-10475-7. doi: 10.1007/978-3-030-10475-7_8-1.

Charles F. Richter. *Elementary Seismology*. W. H. Freeman and Company, Inc., San Francisco, California, 1958.

Alan Ryall and William U. Savage. A comparison of seismological effects for the Nevada Underground Test Boxcar with natural earthquakes in the Nevada region. *Journal of Geophysical Research (1896-1977)*, 74(17):4281–4289, 1969. ISSN 2156-2202. doi: 10.1029/JB074i017p04281.

David P. Schaff and Paul G. Richards. Improvements in magnitude precision, using the statistics of relative amplitudes measured by cross correlation. *Geophysical Journal International*, pages 335–350, 2014. ISSN 0956-540X. doi: 10.1093/gji/ggt433.

Robert Shcherbakov and Donald L. Turcotte. A Modified Form of Båth's Law. *Bulletin of the Seismological Society of America*, 94(5):1968–1975, October 2004. ISSN 0037-1106. doi: 10.1785/012003162.

Peter M. Shearer. Self-similar earthquake triggering, Bath's law, and foreshock/aftershock magnitudes: Simulations, theory, and results for southern California. *Journal of Geophysical Research-Solid Earth*, 117:B06310, June 2012. ISSN 2169-9313. doi: 10.1029/2011JB008957.

Catherine M. Snelson, Robert E. Abbott, Scott T. Broome, Robert J. Mellors, Howard J. Patton, Aviva J. Sussman, Margaret J. Townsend, and William R. Walter. Chemical Explosion Experiments to Improve Nuclear Test Monitoring. *Eos, Transactions American Geophysical Union*, 94(27):237–239, 2013. ISSN 2324-9250. doi: 10.1002/2013EO270002.

Donald L. Springer, Gayle A. Pawloski, Janet L. Ricca, Robert F. Rohrer, and David K. Smith. Seismic Source Summary for All U.S. Below-Surface Nuclear Explosions. *Bulletin of the Seismological Society of America*, 92(5):1806–1840, June 2002. ISSN 0037-1106. doi: 10.1785/0120010194.

Seth Stein and Mian Liu. Long aftershock sequences within continents and implications for earthquake hazard assessment. *Nature*, 462(7269):87–89, November 2009. ISSN 1476-4687. doi: 10.1038/nature08502.

M. Nafi Toksöz and Harold H. Kehrer. Underground Nuclear Explosions: Tectonic Utility and Dangers. *Science*, 173(3993):230–233, July 1971. ISSN 0036-8075, 1095-9203. doi: 10.1126/science.173.3993.230.

M. Nafi Toksöz and Harold H. Kehrer. Tectonic strain-release characteristics of CANNIKIN. *Bulletin of the Seismological Society of America*, 62(6):1425–1438, December 1972. ISSN 0037-1106.

Robert Uhrhammer. Characteristics of northern and southern california seismcity. *Earthquake Notes*, 57(21), 1986.

U.S. Department of Energy. Recommendation by the Secretary of Energy Regarding the Suitability of the Yucca Mountain Site for a Repository under the Nuclear Waste Policy Act of 1982. Technical Report HQO.20020352.0002, Yucca Mountain Project, Las Vegas, Nevada, February 2002.

David H. von Seggern and James N. Brune. Seismicity in the Southern Great Basin, 1868–1992. In *Geologic and Geophysical Characterization Studies of Yucca Mountain, Nevada, A Potential High-Level Radioactive-Waste Repository*, number 058 in U.S. Geological Survey Digital Data Series. U.S. Geological Survey, Washington, D.C., 2000. ISBN 0-607-94822-1.

William R. Walter, Kevin Mayeda, and Howard J. Patton. Regional seismic observations of the Non-Proliferation Experiment at the Livermore NTS Network. In *Proceedings of the Symposium on the Non-Proliferation Experiment: Results and Implications for Test Ban Treaties*, Rockville, Maryland, 1994. Department of Energy.

William R. Walter, Douglas A. Dodge, Gene Ichinose, Stephen C. Myers, Michael E. Pasyanos, and Sean R. Ford. Body-Wave Methods of Distinguishing between Explosions, Collapses, and Earthquakes: Application to Recent Events in North Korea. *Seismological Research Letters*, 89(6):2131–2138, November 2018. ISSN 0895-0695. doi: 10.1785/0220180128.

W. H. Westphal. Aftershocks from Underground Nuclear Explosions. Final Report VUP-0607, Stanford Research Institute, Menlo Park, California, 1962.

D. E. Willis, G. D. George, K. G. Poetzl, C. E. Saltzer, A. F. Shakal, R. D. Torfin, T. L. Woodzick, and C. Wolosin. Seismological aspects of the CANNIKIN nuclear explosion. *Bulletin of the Seismological Society of America*, 62(6):1377–1395, December 1972. ISSN 0037-1106. doi: 10.1785/BSSA0620061377.

I G Wong, R K Green, J I Sun, S K Pezzopane, N A Abrahamson, and R C Quittmeyer. A preliminary assessment of earthquake ground shaking hazard at Yucca Mountain, Nevada and implications to the Las Vegas region. In *Report Number: ANL/TM-YO484-97; CONF-9611220-*, Research Org.: TRW, Inc., Fairfax, VA (United States), December 1996.

Ivan G. Wong and Carl Stepp. Probalistic Seismic Hazard Analysis for Fault Displacement and Vibratory Ground Motion at Yucca Mountain, Nevada, September23, 1998. Final Report MOL.19981207.0393, U.S. Geological Survey, Oakland, California, September 1998.

J. J. Zucca, C. Carrigan, P. Goldstein, S. Jarpe, J. Sweeney, W. L. Pickles, and B. Wright. Signatures of Testing: On-Site Inspection Technologies. In Eystein S. Husebye and Anton M. Dainty, editors, *Monitoring a Comprehensive Test Ban Treaty*, NATO ASI Series, pages 123–134. Springer Netherlands, Dordrecht, 1996. ISBN 978-94-011-0419-7. doi: 10.1007/978-94-011-0419-7_10.

Sean R. Ford
Lawrence Livermore National Laboratory
P.O. Box 808, L-046
Livermore, California 94551-0808

William R. Walter
Lawrence Livermore National Laboratory
P.O. Box 808, L-046
Livermore, California 94551-0808

List of Figures

1 Maximum aftershock analysis for 134 NNSS explosions with at least one aftershock (many events overlay one another). a) Explosion magnitude (m_{main}) versus the largest magnitude aftershock (m_{max}). The dashed lines between $1 \leq (m_{\mathrm{main}} - m_{\mathrm{max}}) \leq 4$ cover about 97% of the events. DAUPHIN and LEYDEN are near the one-to-one line (solid line) where $m_{\mathrm{main}} = m_{\mathrm{max}}$. In both cases the maximum magnitude event is the collapse (filled circles). b) Histogram of magnitude difference between explosion and largest aftershock. The mean is 2.54 and therefore, for the NNSS, Båth's law for explosions is about 2.5 ($\overline{\Delta m_{\mathrm{NTS}}} = 2.54$). 24

2 Vertical (Z), radial (R), and tangential (T) component seismograms of the mainshock explosion (upper traces) and largest aftershock (lower traces) for 3 s in duration (bar in lower right is 1 s) filtered between 1 and 10 Hz. a) SPE-5 mainshock and largest aftershock recorded at station L4006 (600 m from SPE-5 epicenter). The aftershock amplitude is multiplied by a factor of 10^4 relative to the mainshock. b) DAG-2 mainshock and largest aftershock recorded at station G15M0 (1 km from DAG-2 epicenter). The aftershock amplitude is multiplied by a factor of 10^3 relative to the mainshock. 25

3 Probability P of at least one background earthquake with magnitude M in several durations (colored lines) and two areas of radius 100 km (solid) and 10 km (dashed) in the NNSS region. 26

Tables

Table 1: Event information

Name	Time [UTC]	Magnitude
SPE-5 Explosion	2016-04-26T20:49:00	2.00*
SPE Largest Aftershock	2016-04-26T23:57:57	–1.74+
DAG-2 Explosion	2018-12-19T18:45:56	2.33*
DAG Largest Aftershock	2019-01-27T01:22:27	–0.50+

*M_L from University of Nevada, Reno

+From relative amplitude and Equation 11

Figures

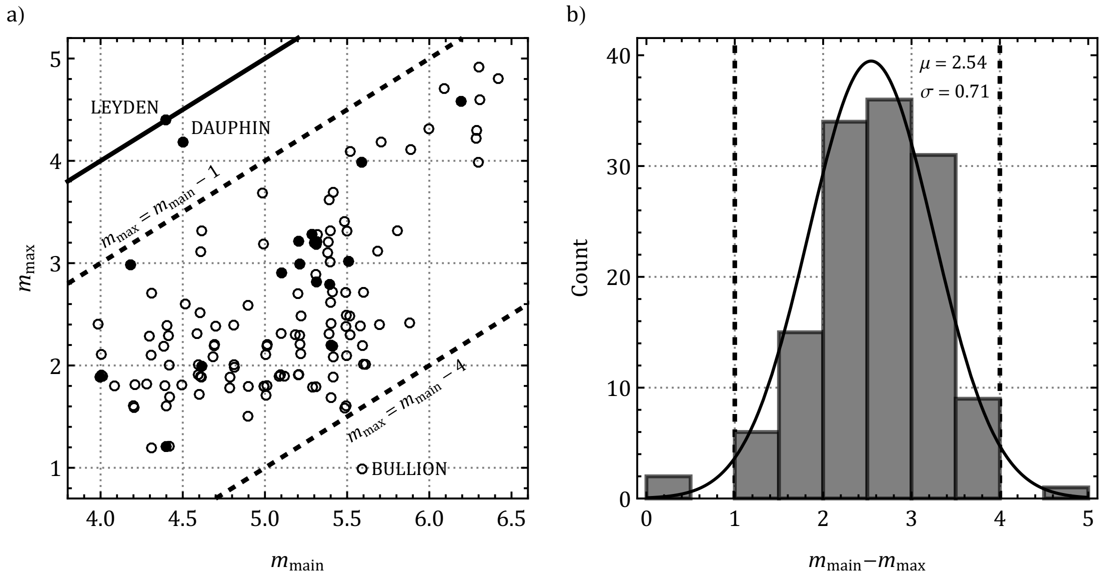

Figure 1: Maximum aftershock analysis for 134 NNSS explosions with at least one aftershock (many events overlay one another). a) Explosion magnitude (m_{main}) versus the largest magnitude aftershock (m_{max}). The dashed lines between $1 \leq (m_{\text{main}} - m_{\text{max}}) \leq 4$ cover about 97% of the events. DAUPHIN and LEYDEN are near the one-to-one line (solid line) where $m_{\text{main}} = m_{\text{max}}$. In both cases the maximum magnitude event is the collapse (filled circles). b) Histogram of magnitude difference between explosion and largest aftershock. The mean is 2.54 and therefore, for the NNSS, Båth's law for explosions is about 2.5 ($\overline{\Delta m_{\text{NTS}}} = 2.54$).

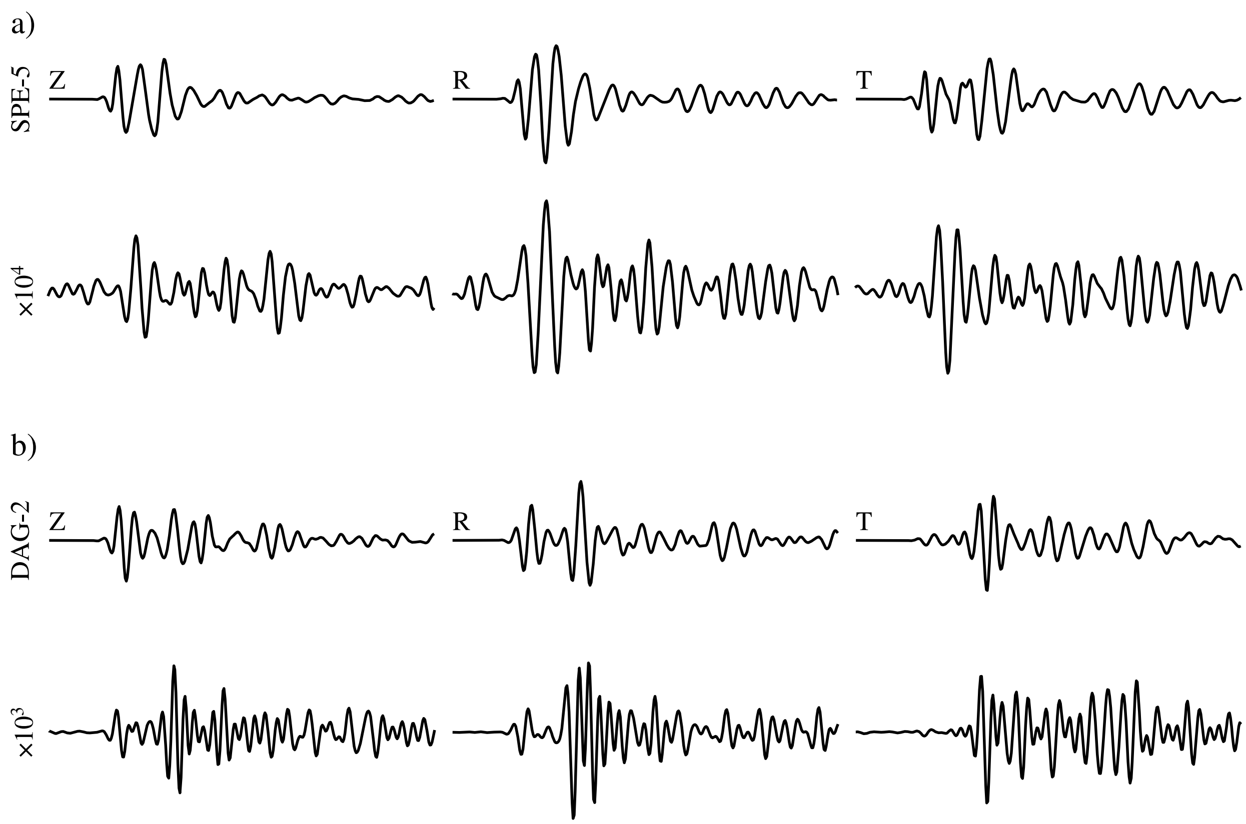

Figure 2: Vertical (Z), radial (R), and tangential (T) component seismograms of the mainshock explosion (upper traces) and largest aftershock (lower traces) for 3 s in duration (bar in lower right is 1 s) filtered between 1 and 10 Hz. a) SPE-5 mainshock and largest aftershock recorded at station L4006 (600 m from SPE-5 epicenter). The aftershock amplitude is multiplied by a factor of 10^4 relative to the mainshock. b) DAG-2 mainshock and largest aftershock recorded at station G15M0 (1 km from DAG-2 epicenter). The aftershock amplitude is multiplied by a factor of 10^3 relative to the mainshock.

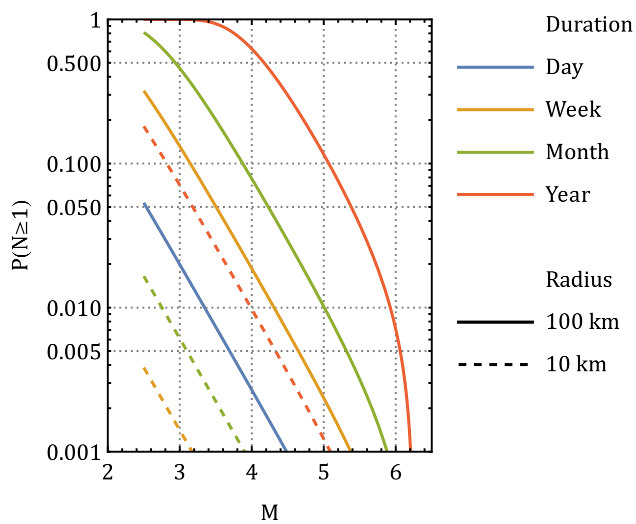

Figure 3: Probability P of at least one background earthquake with magnitude M in several durations (colored lines) and two areas of radius 100 km (solid) and 10 km (dashed) in the NNSS region.